Int. J. Heat Mass Transfer. Vol. 31, No. 11, pp. 2273–2283, 1988
Printed in Great Britain

0017–9310/88 $3.00 + 0.00

The process of melting by rolling contact

ADRIAN BEJAN
Department of Mechanical Engineering and Materials Science, Duke University, Durham, NC 27706, U.S.A.

(*Received* 11 *January* 1988 *and in final form* 6 *April* 1988)

Abstract—This paper describes the fundamentals of the heat transfer melting process occurring in the narrow rolling contact region between a body of phase-change material and a solid body that acts as a heater. The theory is based on the following assumptions: (i) the phase-change material is at the melting point temperature, (ii) the surface of the solid is isothermal, (iii) the effect of frictional heating in the liquid gap is negligible, (iv) the peripheral length of the liquid region is much smaller than the radius of the roller, (v) the liquid gap region is slender, and (vi) the effect of surface tension is negligible. The general solution constructed in this manner relates the mechanical loading of the roller (normal force, tangential force, applied torque) to the angular speed of the roller, the temperature difference between the heater and the phase-change material and the thermophysical properties of the liquid phase. Simpler calculation procedures are developed for two special applications: (a) the melting of a cylinder mounted freely on its axle, and (b) the melting of a turning cylinder the axle of which is stationary relative to the heater surface.

1. INTRODUCTION

THE SUBJECT of this paper is the thin-film melting process that occurs in the narrow strip contact between a solid cylinder rolling on a flat substrate at a different temperature. The solid part that melts will be referred to as the 'phase-change material', and the warmer solid part that does not melt will be referred to as the 'heater'. Figure 1 shows the two configurations in which the problem can be attacked. In Fig. 1(a) a cylinder of phase-change material is shown rolling on the heater surface and leaving a film of liquid on this surface. In Fig. 1(b) the roles are reversed, as the position of the roller is occupied now by the heater and the position of the base by the phase-change material. In this second configuration the end result is the same—a liquid film on the base surface, in the wake of the roller.

The analyst is free to choose between Figs. 1(a) and (b) as frameworks in which to construct a theoretical argument. The analysis reported in this paper happens to be constructed with reference to Fig. 1(a). In both configurations the engineering challenge is the same, namely, to calculate the melting rate of the phase-change material when told the temperature difference and the forces that are maintained between the two solid parts.

The present phase-change heat transfer phenomenon is related to the classical problem of rolling contact with liquid film lubrication. A chronological listing of representative publications in this classical area is given in refs. [1–9]. In the classical rolling contact lubrication problem the shape of the liquid-filled gap is known from the start, as it is fixed by the shape of the roller itself. The problem addressed in this paper is both tougher and more interesting, because the liquid gap shape and size depend not only on the heat transfer rate but also on the mechanical loading of the cylinder. It is shown in Fig. 2 that the loading is represented in general by three quantities, the normal force F_n, the tangential force F_t and the torque M.

2. THE LIQUID GAP SHAPE

Consider the two-dimensional configuration sketched in Fig. 2, in which a horizontal cylinder of phase-change material rolls with a known angular speed along the flat surface of the heater. In a Cartesian system of coordinates (x, y) attached to the base

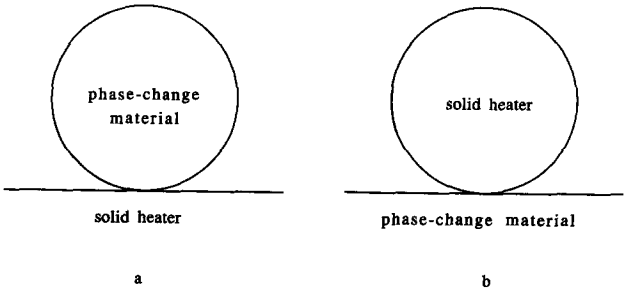

FIG. 1. Two possible configurations for the process of melting by rolling contact.

NOMENCLATURE

B	characteristic dimensionless heat transfer parameter of the rolling contact melting problem, equation (24)
$B_{\min}$	dimensionless viscosity parameter, equation (58)
c	specific heat
C	constant, equation (17)
f_1, f_2	functions, equations (56) and (57)
F_n	normal force [N m^{-1}]
F_{n*}	dimensionless normal force, equation (23)
F_t	tangential force, equation (30)
F_{t*}	dimensionless tangential force, equation (31)
h	liquid gap thickness
Δh	difference between the exit and entrance liquid gap thickness
h_{sf}	latent heat of fusion
k	thermal conductivity of liquid
K_1, K_2	constants, equations (20)
L	half-length of liquid gap
M	applied clockwise torque, equation (33)
M_*	dimensionless torque, equation (35)
P	pressure
$\tilde{P}$	dimensionless pressure group, equation $(18)_2$
q	heat transfer interaction per unit area [J m^{-2}]
Q	height integrated flow rate, $\int_0^h u\,dy$
r	cylinder radius
t	time
T	temperature
ΔT	temperature difference
T_m	melting point temperature
T_s	temperature of the heater (base) surface
u	longitudinal velocity
U	slip speed
$\tilde{U}$	dimensionless slip speed parameter, equation $(18)_3$
v	vertical velocity
V	melting speed, equation (1)
V_*	dimensionless melting speed parameter, equation (25)
x, y	longitudinal and transversal coordinates, Fig. 2
X, Y	dimensionless parameters, $1+\lambda$, $1-\lambda$, respectively.

Greek symbols

α	thermal diffusivity of liquid
λ	dimensionless parameter, $\omega L/V$
μ	viscosity
ξ	dimensionless longitudinal coordinate, equation $(18)_1$
ρ	density of liquid
ϕ_n	function shown on the right-hand side of equation (22)
ϕ_p	function defined in equation (36)
ϕ_t	function shown on the right-hand side of equation (32)
Φ	viscous dissipation function, equation (2)
Φ_n	function defined in equation (45)
Φ_t	function defined in equation (46)
ψ	function, equation (37)
Ψ	function, equation (38)
ω	angular speed.

surface and the center of the cylinder cross-section, a solid base is shown moving to the left and a 'stationary' cylinder rotating clockwise with angular speed ω. Actually, in this frame the cylinder axis is not truly stationary, as it descends slowly with the instantaneous vertical speed

$$V = -\frac{dr}{dt}. \tag{1}$$

The 'melting' speed V is the chief unknown of the problem. This and the other unknowns represented by the forces that must be applied on the melting cylinder in order to roll it with speed ω can only be determined by focusing on the liquid film created by melting in the thin gap of height $h(x)$. This gap has been expanded for better viewing in the right half of Fig. 2.

In order to isolate the rolling contact melting

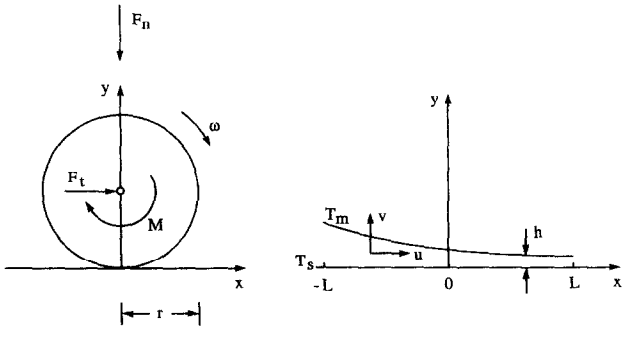

FIG. 2. Mechanical loading and system of coordinates.

phenomenon from other heat transfer processes that might be present in the same configuration (e.g. conduction in the two solid parts), consider the case where the phase-change cylinder is at its melting point (T_m) while the flat solid base is isothermal and at a higher temperature (T_s), i.e. $\Delta T = T_s - T_m > 0$.

The conservation of energy at every point in the liquid gap is accounted for by writing

$$u\frac{\partial T}{\partial x}+v\frac{\partial T}{\partial y}=\alpha\left(\frac{\partial^2 T}{\partial x^2}+\frac{\partial^2 T}{\partial y^2}\right)+\frac{\mu}{\rho c}\Phi \qquad (2)$$

where Φ is the viscous dissipation function and (α, μ, ρ, c) the liquid properties defined in the Nomenclature. A total of four scales compete in the energy balance represented by equation (2), namely, (i) the convection effect (the left-hand side of the equation), (ii) the effect of longitudinal conduction, (iii) the effect of transversal conduction and (iv) the volumetric frictional heating effect

$$\omega r\frac{\Delta T}{L},\quad \alpha\frac{\Delta T}{L^2},\quad \alpha\frac{\Delta T}{h^2},\quad \frac{\mu}{\rho c}\left(\frac{\omega r}{h}\right)^2. \qquad (3)$$

The analysis that follows is based on the important assumption that the dominating effect in the energy balance (2) is that of transversal conduction. This assumption is equivalent to assuming three things simultaneously, first, negligible convection relative to transversal conduction

$$\frac{\omega r h^2}{\alpha L}\ll 1 \qquad (4)$$

second, negligible longitudinal conduction

$$\frac{h}{L}\ll 1 \qquad (5)$$

and, third, negligible frictional heat generation

$$\frac{\mu(\omega r)^2}{k\Delta T}\ll 1. \qquad (6)$$

At this point one relies on assumptions (4)–(6) in order to simplify equation (2) to the statement that the temperature distribution across the liquid-filled gap is linear. Integrated subject to the boundary conditions $T(y=0)=T_s$ and $T(y=h)=T_m$, equation (2) yields the temperature profile

$$T=T_m+\Delta T\left(1-\frac{y}{h}\right). \qquad (7)$$

As in other phase-change heat transfer problems, the position of the two-phase interface is fixed by the energy balance at the interface, which in this case reads

$$-k\left(\frac{dT}{dy}\right)_{y=h}=\rho h_{sf}(-v)_{y=h}. \qquad (8)$$

In this equation $(-v)_{y=h}$ represents the downward velocity with which the melt enters the liquid region of height h and unknown length $2L$. By considering the geometry and kinematics of the rolling cylinder it is easy to show that if the liquid gap is short when compared with the cylinder radius

$$\frac{L}{r}\ll 1 \qquad (9)$$

the downward velocity with which the solid phase-change material approaches the interface is $(V+\omega x)$. The conservation of mass across the interface requires then

$$(-v)_{y=h}=V+\omega x \qquad (10)$$

where it has been assumed that the densities of the liquid and solid phases of the phase-change material are practically equal. Combining equations (7), (8) and (10) one obtains

$$h(x)=\frac{k\Delta T}{\rho h_{sf}(V+\omega x)}. \qquad (11)$$

This result shows that the gap height decreases monotonically as x increases, that is, towards the 'entrance' to the rolling contact region. This feature has been sketched already in Fig. 2 (the right-hand side).

3. THE NORMAL FORCE

Next, attention is turned to the manner in which the flow of the liquid film through the gap provides the pressure build-up necessary for supporting the normal forces applied on the cylinder axis. One begins with the classical simplified momentum equation of thin-film lubrication theory (see, e.g. Batchelor [10])

$$\frac{\partial^2 u}{\partial y^2}=\frac{1}{\mu}\frac{dP}{dx} \qquad (12)$$

which is based on the assumptions of negligible longitudinal inertia and that of a slender enough liquid domain. Note that the latter has been assumed already in writing equation (5). Integrating now equation (12) subject to the rolling velocity conditions, $u(h)=-\omega r$ and $u(0)=-\omega r-U$, one obtains

$$u=\frac{1}{2\mu}\left(\frac{dP}{dx}\right)y(y-h)-\omega r+U\left(\frac{y}{h}-1\right). \qquad (13)$$

In this velocity profile expression U represents the 'slip speed', that is, the relative speed between the roller and the base.This terminology means that relative to the base the cylinder axis moves in the direction of F_t with speed $(\omega r+U)$, while the lowest point of the cylinder slides in the same direction with speed U.

A more useful quantity is the height-integrated flow rate $Q(x)$ (see Nomenclature), which, in view of equation (13), means

$$Q=-\frac{h^3}{12\mu}\frac{dP}{dx}-h\omega r-\frac{hU}{2}. \qquad (14)$$

A second equation for Q follows from the mass continuity equation for the liquid gap

$$\frac{\partial u}{\partial x}+\frac{\partial v}{\partial y}=0 \tag{15}$$

which, integrated first from $y=0$ to h, and later in x, yields

$$Q=-\omega rh+Vx+\tfrac{1}{2}\omega x^2+\text{constant}. \tag{16}$$

The integration in the y-direction is based on invoking boundary condition (10) at $y=h$, the impermeable base condition $v=0$ at $y=0$, and Leibnitz' formula for differentiation under the integral sign, while keeping in mind that h is a function of x.

Eliminating the flow rate $Q(x)$ between equations (14) and (16) one obtains an expression for the pressure gradient along the liquid filled gap

$$\frac{1}{12}\frac{\mathrm{d}\tilde{P}}{\mathrm{d}\xi}=-C(1+\xi)^3-\xi\left(1+\frac{\xi}{2}\right)(1+\xi)^3-\frac{\tilde{U}}{2}(1+\xi)^2 \tag{17}$$

where

$$\xi=\frac{\omega x}{V},\quad \tilde{P}=P\frac{\omega^2}{\mu}\left(\frac{k\Delta T}{\rho h_{sf}V^2}\right)^3 \quad\text{and}\quad \tilde{U}=U\frac{\omega k\Delta T}{\rho h_{sf}V^3}. \tag{18}$$

The undetermined constant C appearing in equation (17) is proportional to the constant introduced in equation (16). Integrating equation (17) one obtains

$$\tilde{P}(\xi)=K_1(1+\xi)^4-(1+\xi)^6-2\tilde{U}(1+\xi)^3+K_2 \tag{19}$$

in which K_1 accounts for the constant C, and where K_2 is a new constant.

Regarding now the pressure P as the difference between the liquid pressure and the background pressure of the surroundings, constants K_1 and K_2 can be determined by setting $\tilde{P}(\lambda)=0=\tilde{P}(-\lambda)$. In other words, the effect of surface tension is assumed to be negligible. One obtains

$$K_1=\frac{X^6-Y^6+2\tilde{U}(X^3-Y^3)}{X^4-Y^4}\quad\text{and}$$

$$K_2=\frac{-(1-\lambda^2)^4+\tilde{U}(1-\lambda^2)^3}{2(1+\lambda^2)} \tag{20}$$

where λ is the dimensionless group $\lambda=\omega L/V$, and where $X=1+\lambda$ and $Y=1-\lambda$.

The pressure integral must equal the net downward force F_n, which is one of the quantities that must be specified in the problem statement

$$F_n=\int_{-L}^{L}P\,\mathrm{d}x. \tag{21}$$

Performing integral (21) one obtains

$$F_{n^*}\frac{B^3}{V_*^7}=\frac{1}{5}K_1(X^5-Y^5)-\frac{1}{7}(X^7-Y^7)-\frac{\tilde{U}}{2}(X^4-Y^4)+2\lambda K_2 \tag{22}$$

where F_{n^*} is the dimensionless notation for the known normal force

$$F_{n^*}=\frac{F_n}{\mu\omega r}. \tag{23}$$

This formulation reveals also an entirely new dimensionless group, B, which is the characteristic heat transfer parameter of the rolling melting process

$$B=\frac{k\Delta T}{\rho h_{sf}\omega r^2}. \tag{24}$$

Finally, the dimensionless parameter V_* accounts for the unknown melting speed

$$V_*=\frac{V}{\omega r}. \tag{25}$$

It is important to note at this juncture that B, V_* and λ are related through a purely kinematic constraint. This relation is based on the observation that the positive gap height difference $\Delta h=h(-L)-h(L)$ is related to the downward movement of the center of the cylinder. Indeed, one can view the rolling contact region (the liquid gap) as a cutting tool that removes steadily a solid 'chip' of radial thickness Δh. It follows that the center of the cylinder travels a distance Δh toward the base plane during one revolution, that is, $\Delta h=2\pi V/\omega$. Evaluating Δh by using equation (11), it is easy to show that this kinematic condition is

$$\frac{B}{V_*^2}=\frac{\pi}{\lambda}(1-\lambda^2). \tag{26}$$

The parameter λ can be written alternatively as

$$\lambda=\frac{L_*}{V_*} \tag{27}$$

where L_* is the dimensionless half length of the liquid gap

$$L_*=\frac{L}{r}. \tag{28}$$

Note that according to assumption (9) this dimensionless length must be smaller than one, in other words

$$L_*\ll 1\quad\text{or}\quad \lambda V_*\ll 1. \tag{29}$$

4. THE TANGENTIAL FORCE

The F_t force that pushes the cylinder axis from left to right in Fig. 2 must be balanced by the total horizontal shear force felt by the same cylinder over the wet spot

$$F_t=\int_{-L}^{L}\mu\left(\frac{\partial u}{\partial y}\right)_{y=h}\mathrm{d}x. \tag{30}$$

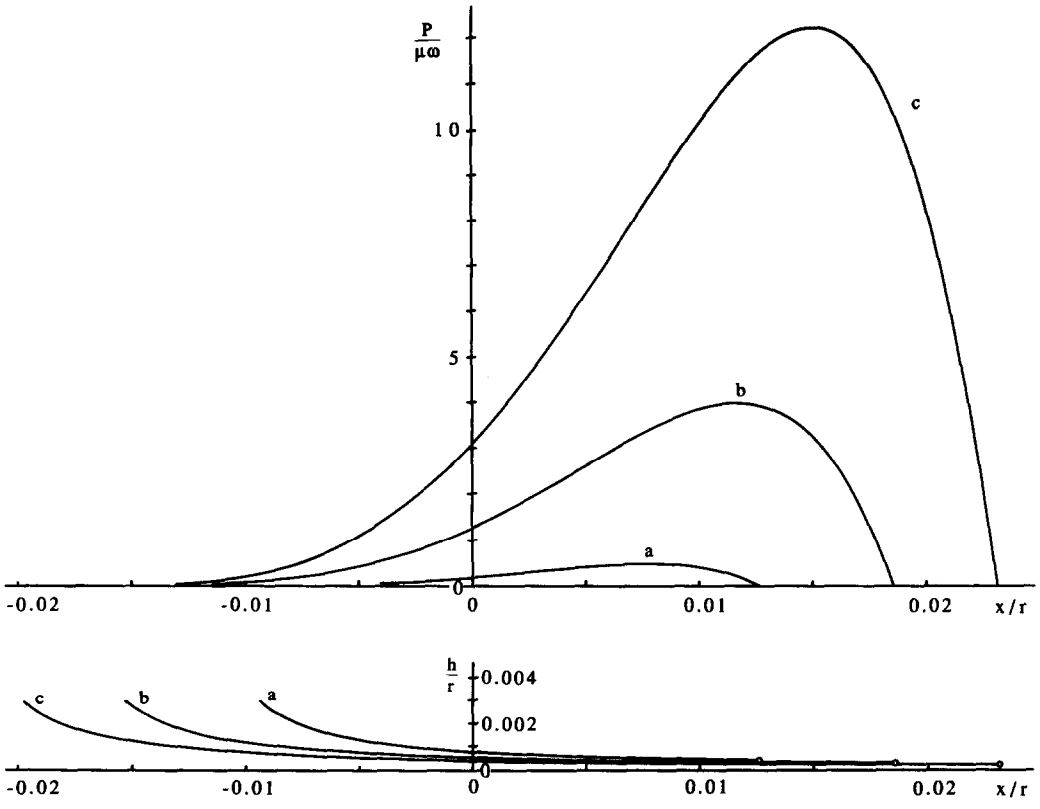

FIG. 3. The pressure distribution in the liquid gap formed by a cylinder mounted freely on its axle, and the corresponding liquid gap shape ($B = 10^{-5}$): (a) $F_{n^*} = 464.5$ (or $\tilde{U} = -1$); (b) $F_{n^*} = 5532$ (or $\tilde{U} = 0$); (c) $F_{n^*} = 20\,168$ (or $\tilde{U} = 1$).

The resulting expression for the dimensionless tangential force

$$F_{t^*} = \frac{F_t}{\mu\omega r} \tag{31}$$

can be summarized as follows:

$$\frac{F_{t^*}B^2}{V_*^5} = \frac{2}{3}K_1(X^3 - Y^3) - \frac{3}{5}(X^5 - Y^5) - \tilde{U}(X^2 - Y^2). \tag{32}$$

5. THE ROTATIONAL EQUILIBRIUM CONDITION

The roller may be driven in general by a combination of translational push (F_t) and the turning of the roller around its axis. The latter requires the application of the torque M, which in Fig. 2 is defined positive when pointing in the clockwise direction. If the rolling process is to proceed with zero angular acceleration, the torque M must always be balanced by the other effects that tend to turn the roller. One such effect is the moment rF_t, which acts in the clockwise direction. Another effect is the moment due to the pressure excess in the liquid gap, because, in general, the F_n resultant of this pressure distribution does not fall precisely on the vertical line that passes through the center of the roller cross-section (Fig. 3).

The rotational equilibrium condition that accounts for all these effects is

$$M + F_t r = \int_{-L}^{L} xP\,dx. \tag{33}$$

In view of equations (31) and (19), this condition means

$$M_* + F_{t^*} = \frac{V_*^8}{B^3}\phi_p \tag{34}$$

in which M_* is the dimensionless applied torque

$$M_* = \frac{M}{\mu\omega r^2} \tag{35}$$

and the function $\phi_p(\lambda, \tilde{U})$ is shorthand for

$$\phi_p(\lambda, \tilde{U}) = \frac{K_1}{6}(X^6 - Y^6) - \frac{1}{8}(X^8 - Y^8) - \frac{2}{5}\tilde{U}(X^5 - Y^5) + \frac{K_2}{2}(X^2 - Y^2) - \phi_n(\lambda, \tilde{U}). \tag{36}$$

The additional function $\phi_n(\lambda, \tilde{U})$ is shorthand notation for the entire right-hand side of equation (22).

6. ANALYTICAL SUMMARY

The analytical conclusions reached in the preceding four sections constitute a sufficient set for determining the melting speed V when 'accessible' parameters such as F_n, F_t, M, ΔT and the geometric and thermophysical properties are specified. Worth noting is that the angular speed ω is also an unknown, because it cannot be specified if F_n, F_t, M, ΔT and all the properties are already known. The same can be said about the slip speed U.

It pays to review the unknowns of the problem *vis-à-vis* the chief analytical results that have been developed so far. There are *four* equations, namely, equations (22), (26), (32) and (34), which relate seven dimensionless parameters, F_{n^*}, F_{t^*}, M_*, B, λ, $\tilde{U}$, and V_*. One could, in principle, eliminate three of these parameters (say, λ, U and V_*) between the four equations, leaving in the end a single equation of the form

$$\psi(F_{n^*}, F_{t^*}, M_*, B) = 0. \tag{37}$$

However, in view of the definitions of the four surviving dimensionless parameters, this single equation is equivalent to

$$\Psi(F_n, F_t, M, \Delta T, \omega, \text{properties}) = 0. \tag{38}$$

This last form illustrates the physical argument made in the preceding paragraph, namely, that one cannot specify ω independently of the mechanical loading (F_n, F_t, M) and the heat transfer configuration (ΔT, properties).

Going back to the dimensionless form (37), one can conclude that one has the freedom to select as many as three dimensionless parameters independently. Any dimensionless unknown (e.g. V_*) is in general a function of three independent parameters. One can see that with a little ingenuity (Section 8) one will be able to condense the solution to this three-degrees-of-freedom problem into a set of two-dimensional charts.

7. CYLINDER MOUNTED FREELY ON ITS AXLE

A very simple construction of the 'melting by rolling' apparatus sketched in Fig. 2 consists of a roller that is mounted freely on an axle. In this case M remains equal to zero as the cylinder rolls along the flat substrate solely under the influence of the translational push F_t and the normal force F_n.

Reviewing the preceding analysis one can see that the $M_* = 0$ condition affects only equation (34), which now reads

$$\frac{V_*^3}{B} = \frac{\phi_t(\lambda, \tilde{U})}{\phi_p(\lambda, \tilde{U})}. \tag{39}$$

The new function $\phi_t(\lambda, \tilde{U})$ is shorthand notation for the expression shown on the right-hand side of equation (32). With M_* being now fixed, the problem is left with only two degrees of freedom. These are represented best by the parameters λ and $\tilde{U}$, which can be selected at will and substituted on the right-hand side of each of equations (22), (26), (32) and (39). For each (λ, $\tilde{U}$) pair one can solve this system of four equations and calculate V_*, B, F_{n^*}, and F_{t^*}.

The solution was accomplished numerically by first combining equations (26) and (39) and solving for V_* and B. With these new values (plus the assumed λ and $\tilde{U}$) one proceeds to equation (22) in order to calculate F_{n^*} and, finally, to equation (32) in order to determine F_{t^*}. Some of the results of this operation are presented in Figs. 3–5.

Figures 3 and 4 illustrate the liquid gap shape and the distributions of pressure and longitudinal velocity in the gap. All the curves are drawn for cases along the constant-B 'isotherm' $B = 10^{-5}$ of the surface (37). The pressure increases steadily as the normal force increases. At the same time the length of the liquid gap increases. The pressure is considerably higher along the upstream half of the gap: this distribution is responsible for the counterclockwise moment recognized in equation (33). Thinking of the roller as a whole, one may say that the roller 'walks on its toes'.

Immediately below the longitudinal pressure profiles one can see the corresponding shapes of the liquid gap region. These shapes are drawn to scale (note the use of the roller radius as length unit in both the horizontal and the vertical directions). The liquid gap becomes increasingly slender as the normal force increases. Worth noting is that the $B = 10^{-5}$ case illustrated here is close to the limit of the least slender (most robust) gaps for which numerical solutions could be obtained. This case was chosen for the purpose of illustration, because infinitely slender gaps are more difficult to draw (and see!) than a gap the height of which is comparable with its length. The liquid gap shapes become more slender as the normal force increases.

Figure 4 shows the longitudinal velocity profiles that correspond to the curves presented in Fig. 3. The velocity profiles are drawn at two longitudinal stations, namely, in the vertical plane that passes through the center of the roller, $\xi = 0$, and in the plane of the gap entrance, $\xi = \lambda$. These two stations contain between them the region of maximum pressure (Fig. 3(top)): this explains the opposing curvatures of the two sets of profiles. Note also that the longitudinal velocities increase as the normal force (or tangential force) increases. At the same time the slip speed between the bottom and top walls of the liquid gap increases.

8. PRESENTATION OF THE RESULTS IN THE LIMIT $\lambda \to 1$

One of the simplifying assumptions on which the preceding theory was based, equation (9) or equation (29), requires that the order of magnitude of λV_* be less than one. Another assumption is that the liquid gap is a slender space, equation (5)

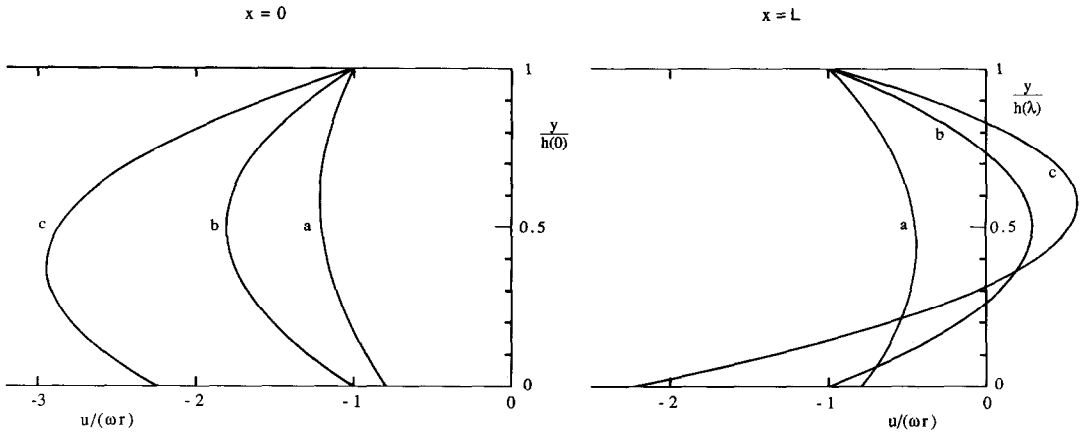

FIG. 4. Longitudinal velocity profiles for cases (a)–(c) described in the caption of Fig. 3.

$$\frac{h}{L} \sim \frac{B}{\lambda V_*^2} \ll 1. \tag{40}$$

The numerical solutions described in the preceding section were generated by varying λ and $\tilde{U}$ independently. The effect of λ and $\tilde{U}$ on the two 'slenderness' criteria recognized above is presented in Fig. 5. The permissible $(\lambda, \tilde{U})$ domain shrinks as one convenes on increasingly stricter (smaller) threshold values for the scales of λV_* and $B/(\lambda V_*^2)$. The numerical solution (omitted here) showed that the highest B order of magnitude for which the solution respects both criteria is 10^{-4}.

The useful aspect of Fig. 5 is that it demonstrates that the $M_* = 0$ solution of Figs. 3 and 4 positions itself in the limit $\lambda \to 1$. In this limit the problem loses one of its degrees of freedom, which means that equation (37) can be represented by a single curve in a plane. The physical meaning of this limit can be seen by rewriting equation (11) as

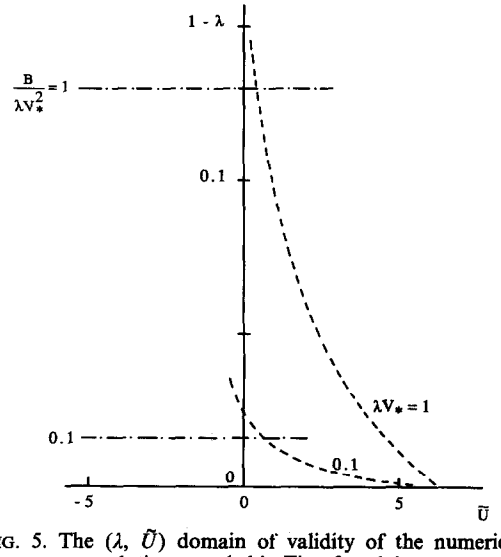

FIG. 5. The $(\lambda, \tilde{U})$ domain of validity of the numerical solution sampled in Figs. 3 and 4.

$$h(x) = \frac{k\Delta T}{\rho h_{sf} V(1+\xi)} \tag{41}$$

in which $(1+\xi)$ varies from $1+\lambda \cong 2$ at the liquid gap entrance to $1-\lambda \ll 1$ at the exit. In conclusion, although in the $\lambda \to 1$ limit the liquid gap is remarkably slender (Fig. 5), the exit cross-section flares out to a height that is considerably larger than the average height of the liquid gap region.

Subjecting the $M_* = 0$ problem of the previous section to the calculus of limits, for the limit $\lambda \to 1$ one obtains

$$\frac{F_{n^*} B^3}{V_*^7} = \frac{8}{5}\left(\frac{32}{7} - \tilde{U}\right) \tag{42}$$

$$\frac{F_{t^*} B^2}{V_*^5} = \frac{4}{3}\left(\frac{8}{5} + \tilde{U}\right) \tag{43}$$

$$\tilde{U} = \frac{44}{7}\left(\frac{V_*^3}{B} - \frac{7}{11}\right)\left(\frac{V_*^3}{B} + \frac{5}{2}\right)^{-1}. \tag{44}$$

These equations replace, in order, equations (22), (32) and (39). The lone degree of freedom in this limit is represented by $\tilde{U}$ or, according to equation (44), the new group V_*^3/B. Note that the left-hand side of equation (42) can be rewritten as $F_{n^*} B^{2/3} (B/V_*^3)^{7/3}$. Taken together, equations (42) and (44) state that

$$F_{n^*} B^{2/3} = \Phi_n\left(\frac{V_*^3}{B}\right). \tag{45}$$

After a similar manipulation, equations (43) and (44) combine into

$$F_{t^*} B^{1/3} = \Phi_t\left(\frac{V_*^3}{B}\right). \tag{46}$$

By varying V_*^3/B in equations (45) and (46) one can obtain a unique curve in the new plane $F_{n^*} B^{2/3} - F_{t^*} B^{1/3}$. This result is shown in Fig. 6. Plotted along this curve is the value of the parameter $V_*/B^{1/3}$. Along the dashed-line portion of the solution the system

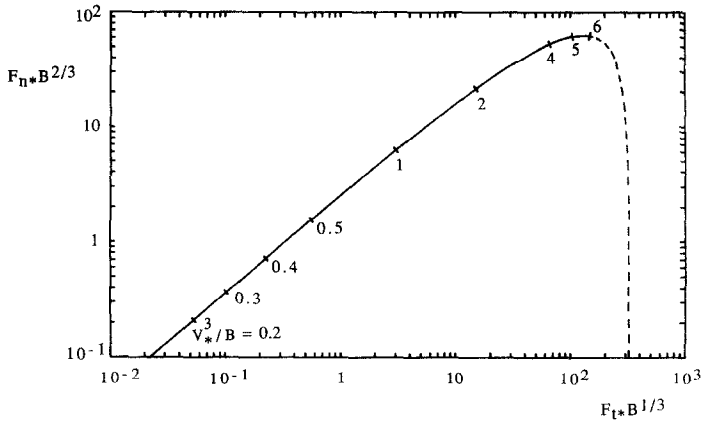

FIG. 6. Single-curve solution for the rolling contact melting of a cylinder mounted freely on its axle.

promises to be mechanically unstable: for example, at constant B, the melting speed increases as the normal force decreases.

Compared with the three-parameter chart that can be drawn based on equation (37) with $M_* = 0$, the asymptotic 'correlation' of Fig. 6 makes it easier to predict unknowns such as the angular speed (ω) and slip speed (U) when F_n, F_t, ΔT and the properties are specified. In fact, all that is needed for calculating ω analytically is a power-law approximation of the solid-line portion of the curve. For example, the $V_*^3/B \to 0$ asymptote of this curve is represented by

$$F_{n*}B^{2/3} \to \frac{1728}{175}\left(\frac{V_*^3}{B}\right)^{7/3} \tag{47}$$

$$F_{t*}B^{1/3} \to \frac{736}{175}\left(\frac{V_*^3}{B}\right)^{8/3} \tag{48}$$

or, after eliminating V_*^3/B, by

$$F_{n*}^{8/7}F_{t*}^{-1}B^{3/7} \to 3.2564. \tag{49}$$

Recalling finally the definitions of the dimensionless parameters, expression (49) provides a formula for relating ω to the physical quantities that can be specified in the problem statement

$$\omega \to 0.1267\left(\frac{F_t}{\mu r}\right)^{-7/4}\left(\frac{F_n}{\mu r}\right)^{2}\left(\frac{k\Delta T}{\rho h_{sf} r^2}\right)^{3/4}. \tag{50}$$

More accurate estimates for ω can be made by using in place of equations (47)–(49) the power-law approximation of the appropriate segment of the solid-line curve on which the operating point (or the V_*^3/B value) falls.

Another result that is hidden in the solution displayed in Figs. 3–6 is the size of the slip speed U. This is, of course, proportional to the dimensionless parameter $\tilde{U}$. It is easy to show that the ratio between the slip speed and the peripheral speed of the roller is

$$\frac{U}{\omega r} = \tilde{U}\frac{V_*^3}{B}. \tag{51}$$

In view of equation (44), the $U/(\omega r)$ ratio emerges as a function of the same lone parameter V_*^3/B on which the single-curve correlation of Fig. 6 is based.

Figure 7 shows the manner in which $U/(\omega r)$ varies with the abscissa parameter of Fig. 6. The slip speed increases well above ωr as the abscissa parameter $F_{t*}B^{1/3}$ as well as the group V_*^3/B assume values that are greater than one. In the opposite extreme the slip speed is, in relative terms, negligible. As shown in the enlarged detail of Fig. 7, the slip speed becomes negative in the range $F_{t*}/B^{1/3} \lesssim 1$. A negative and small $U/(\omega r)$ ratio means that the translational speed of the cylinder ($\omega r + U$) is slightly less than its peripheral speed (ωr).

One final observation concerns the two slenderness conditions (29) and (40), which must be respected as $\lambda \to 1$. In this limit these conditions produce two simpler inequalities

$$B^{1/2} \ll V_* \ll 1. \tag{52}$$

In conclusion, the operating conditions represented by a point on the single curve of Fig. 6 must be such that V_* and B are individually smaller than one and, in addition, B is smaller than V_*^2. These conditions do not restrict the range of values that is allowed for the lone parameter V_*^3/B, with which one was able to describe the curve of Fig. 6. Equation (52) can easily be rewritten as

$$B^{1/2} \ll \frac{V_*^3}{B} \ll B^{-1} \tag{53}$$

to show that the group V_*^3/B is allowed to assume values that are smaller or greater than one (recall that $B \ll 1$).

9. STATIONARY CYLINDER

As a second problem consider the case of a cylinder the axis of which does not move along the flat heater. The cylinder rotates in place under the influence of F_n, F_t and M, while the melting process removes a steady film of liquid from the cylinder periphery. This problem is represented by the kinematic condition

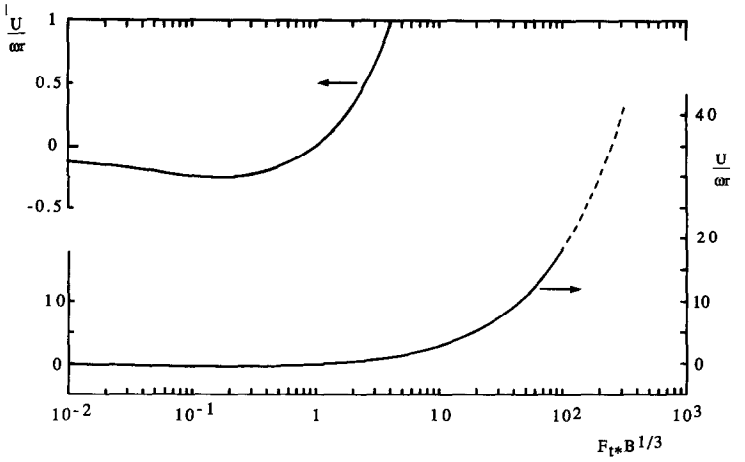

FIG. 7. The slip speed between the bottom of the phase-change roller and the flat heater.

$u(0) = 0$, which means that $U/(\omega r) = -1$, or, in view of equation (51)

$$\tilde{U} = -\frac{B}{V_*^3}. \tag{54}$$

Educated by the asymptotic solution developed in the preceding section, one can invoke from the outset the limit $\lambda \to 1$. In this limit the general rotational equilibrium condition (34) reduces to

$$\tilde{U} = \frac{44}{7}\left[\frac{V_*^3}{B} - \frac{7}{11} - \frac{105}{352}M_* B^{1/3}\left(\frac{B}{V_*^3}\right)^{5/3}\right]\left(\frac{V_*^3}{B} + \frac{5}{2}\right)^{-1}. \tag{55}$$

It is worth noting that equation (44) is the special 'zero-moment' limit of equation (55). Note further that the vertical and longitudinal force balances (45) and (46) apply unchanged to the present problem.

The solution to the stationary cylinder problem can be obtained parametrically by combining equations (45), (46) and (55). The role of 'parameter' is played by the group V_*^3/B (or by $\tilde{U}$, equation (54)). The results are presented in Figs. 8 and 9. Assuming that the temperature difference parameter B is fixed, from Fig. 8 one can learn that both the melting speed V_* and the applied moment M_* increase as the normal force increases. The behavior of $M_* B^{1/3}$ at small values of the abscissa parameter $F_{n*}B^{2/3}$ is illustrated in Fig. 9.

The tangential force F_{t*} exhibits a somewhat more interesting behavior (Figs. 8 and 9). It increases with the normal force only in the domain where the abscissa parameter $F_{n*}B^{2/3}$ is greater than approximately 0.5. Furthermore, there exists a critical condition represented by $V_*^3/B = 0.625$ or $F_{n*}B^{2/3} = 3.3$, where the tangential force is zero. In the 'light pressure' domain $F_{n*}B^{2/3} < 3.3$ the tangential force is small and negative, meaning that the operator of the device must pull the cylinder in the negative x-direction, while turning it clockwise and pressing it downward.

The preceding results are based on the slenderness assumptions (29) and (40), which for the $\lambda \to 1$ limit have been summarized in expression (53). This expression and the V_*^3/B curve of Fig. 8 show that the domain of validity of the plotted results becomes in-

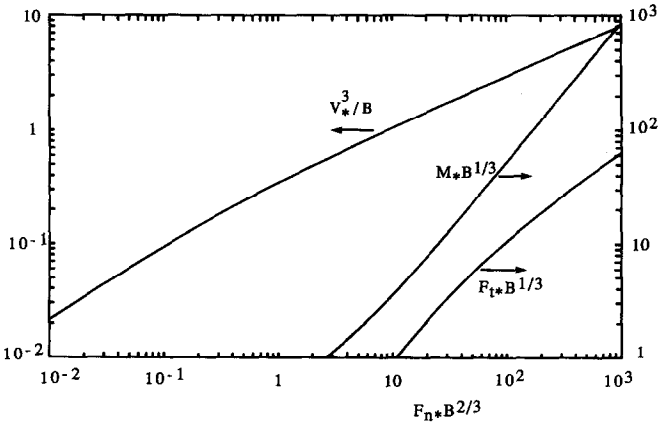

FIG. 8. Solution for the rolling contact melting of a stationary cylinder.

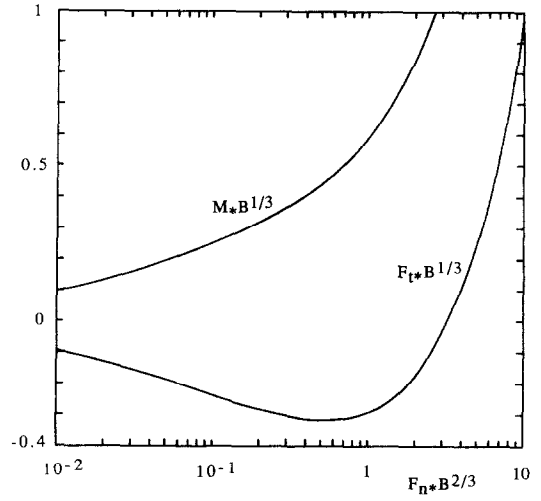

FIG. 9. The behavior of the solution of Fig. 8 in the limit of light pressures (small normal forces).

creasingly wider as the temperature difference parameter B decreases.

10. CONCLUDING REMARKS

The work assembled in this paper consists of first developing a general theory for the rolling contact melting process (Sections 2–6) and later solving two specific problems, the freely spinning roller (Sections 7 and 8) and the cylinder that rolls while standing still (Section 9). The solutions to these two problems demonstrated the usefulness and validity of invoking the limit $\lambda \to 1$. In closing, it pays to take another look at the most general theory (Sections 2–6).

In the $\lambda \to 1$ limit the general theory reduces to a set of three equations, equations (45), (46) and (55), with which one can calculate three groups, respectively, $F_{n*}B^{2/3}$, $F_{t*}B^{1/3}$ and $M_*B^{1/3}$. The equations show that each of these groups is a function of two parameters, namely, $\tilde{U}$ and V_*^3/B. Eliminating $\tilde{U}$ between the three equations one can reduce the problem to the calculation of two surfaces, one for the relationship between the mechanical loads

$$M_*B^{1/3} = f_1(F_{n*}B^{2/3}, F_{t*}B^{1/3}) \tag{56}$$

and the other for the melting speed

$$\frac{V_*^3}{B} = f_2(F_{n*}B^{2/3}, F_{t*}B^{1/3}). \tag{57}$$

These surfaces can be obtained numerically in the way in which one handled the special cases of Sections 8 and 9. For example, the single curve of Fig. 6 is the projection on the base plane $F_{n*}B^{2/3}$–$F_{t*}B^{1/3}$ of the intersection between the plane $M_*B^{1/3} = 0$ and the surface represented by equation (56).

In conclusion, in the limit $\lambda \to 1$ the number of degrees of freedom of the problem decreases to two. Raised to the power 1/3 or 2/3, the heat transfer parameter B participates only as a scaling factor in the construction of new dimensionless groups for the normal force, tangential force, applied torque and melting speed.

Worth keeping in mind is that the slenderness criteria (53) identify the regions of surfaces (56) and (57) in which that solution is valid. The regions become increasingly wider as B becomes considerably smaller than one. It turns out, however, that the heat transfer parameter B cannot decrease indefinitely without threatening the foundations of the theory. This feature is due to the neglect of the effect of frictional heating in the liquid gap, equation (6), which is equivalent to assuming that $\mu\omega/(\rho h_{sf}) < B$. This limitation reveals another important heat transfer parameter of the rolling melting process

$$B_{\min} = \frac{\mu\omega}{\rho h_{sf}}. \tag{58}$$

Therefore, the present theory holds for the 'sufficiently small' viscosities recommended by $B_{\min} < B$.

Implicit in this entire work is also the assumption that the elastic deformation of the heater material can be neglected in the description of the liquid gap shape. In accordance with the solution to the Hertz elastic contact problem [12], this assumption means that the modulus of elasticity of the heater material is greater than a certain order of magnitude. In general, the problem is 'elasto-hydrodynamic' [13] as the liquid gap shape is determined by the interplay between the melting and lubrication phenomenon analyzed in this paper and the solid deformation caused by surface pressure distributions such as those displayed in Fig. 3.

Finally, it is worth noting two melting phenomena that are related to the one treated in this paper. The case $\omega = 0$ corresponds to the contact melting of a solid that slides along the heater surface. This particular problem and the one in which the heating is provided by viscous effects in the liquid gap is described in a separate article [14]. The even more restricted case of no rotation ($\omega = 0$) and zero slip ($U = 0$) corresponds to the contact melting problem studied by Bareiss and Beer [15] and Webb *et al.* [16]. These authors studied the melting of a block of ice that stagnates (pushes) against the upper boundary of a horizontal cylindrical capsule.

Acknowledgement—The support received from the National Science Foundation through Grant No. CBT-8711369 is gratefully acknowledged.

REFERENCES

1. O. Reynolds, On rolling friction, *Phil. Trans. Soc.* **166**(1), 155–174 (1875).
2. A. G. M. Michell, *Lubrication*, pp. 213–217. Blackie, London (1950).
3. A. W. Crook, The lubrication of rollers, *Phil. Trans. Soc.* **A250**, 387–409 (1958).
4. J. F. Archard and M. T. Kirk, Lubrication at point contacts, *Proc. R. Soc.* **A261**, 532–550 (1961).
5. T. Sasaki, H. Mori and N. Okino, Fluid lubrication

theory of roller bearing, *ASME J. Basic Engng* **84**, 166–174, 175–180 (1962).
6. D. Dowson, G. R. Higginson and A. V. Whitaker, Stress distribution in lubricated rolling contacts, *Symposium on Fatigue in Rolling Contact, Proceedings*, Paper 6, Institution of Mechanical Engineers, London (1963).
7. P. Castle and D. Dowson, A theoretical analysis of the starved elastohydrodynamic lubrication problem for cylinders in line contact, *Elastohydrodynamic Lubrication 1972 Symposium Proceedings*, Paper C35/72, Institution of Mechanical Engineers, London, 11–13 April (1972).
8. W. J. Anderson, Rolling-element bearings. In *Tribology: Friction, Lubrication and Wear* (Edited by A. Z. Szeri), Chap. 8. Hemisphere, Washington, DC (1980).
9. T. A. Harris, *Rolling Bearing Analysis*, 2nd Edn. Wiley, New York (1984).
10. G. K. Batchelor, *An Introduction to Fluid Dynamics*, pp. 219–222. Cambridge University Press, Cambridge (1967).
11. H. S. Carslaw and J. C. Jaeger, *Conduction of Heat in Solids*, 2nd Edn. Oxford University Press, Oxford (1959).
12. S. P. Timoshenko and J. N. Goodier, *Theory of Elasticity*, 3rd Edn, pp. 409–420. McGraw-Hill, New York (1970).
13. K. T. Yang, Lubrication and thermal effects in metal processing. In *Interdisciplinary Issues in Materials Processing and Manufacturing* (Edited by S. K. Samanta, R. Komanduri, R. McMeeking, M. M. Chen and A. Tseng), Vol. 2, pp. 485–500. Presented at the ASME Winter Annual Meeting, Boston, 13–18 December (1987).
14. A. Bejan, The fundamentals of sliding contact melting and friction, *J. Heat Transfer* (1988), to be published.
15. M. Bareiss and H. Beer, An analytical solution of the heat transfer process during melting of an unfixed solid phase change material inside a horizontal tube, *Int. J. Heat Mass Transfer* **27**, 739–746 (1984).
16. B. W. Webb, M. K. Moallemi and R. Viskanta, Experiments on melting of unfixed ice in a horizontal cylindrical capsule, *J. Heat Transfer* **109**, 454–459 (1987).

LE MECANISME DE FUSION PAR CONTACT FROTTANT

Résumé—On décrit les bases du mécanisme de fusion qui se produit dans la même région de contact entre un corps à changement de phase et un solide qui agit comme chauffoir. La théorie est basée sur les hypothèses suivantes: (i) le matériau à changement de phase est à la température du point de fusion, (ii) la surface du solide est isotherme, (iii) l'effet du chauffage par frottement dans l'espace liquide est négligeable, (iv) la longueur périphérique de la région liquide est plus petite que le rayon du rouleau, (v) l'épaisseur de la région liquide est mince et (vi) l'effet de la tension interfaciale est négligeable. La solution générale construite de cette façon relie la charge mécanique du rouleau (forces normale et tangentielle, couple appliqué) à la vitesse angulaire du rouleau, à la différence de température entre le chauffoir et le matériau à changement de phase et aux propriétés thermophysiques de la phase liquide. Des procédures de calcul simples sont développées pour deux applications spéciales: (a) la fusion d'un cylindre monté libre sur son axe et (b) la fusion d'un cylindre tournant dont l'axe est fixe par rapport à la surface du chauffoir.

EIN SCHMELZVERFAHREN MIT ROTIERENDER KONTAKTFLÄCHE

Zusammenfassung—Diese Veröffentlichung beschreibt die Grundlagen der Wärmeübertragung beim Schmelzprozeß in der schmalen rotierenden Kontaktschicht zwischen einem Körper mit Phasenübergang und einem beheizten Festkörper. Die Theorie basiert auf den folgenden Annahmen: (i) das Material, welches den Phasenwechsel vollzieht, besitzt Schmelztemperatur, (ii) die gesamte Oberfläche des Feststoffes hat eine einheitliche Temperatur, (iii) der Effekt der Reibungswärme in dem mit Flüssigkeit gefüllten Spalt ist vernachlässigbar, (iv) die tangentiale Ausdehnung der Flüssigkeitsschicht ist viel kleiner als der Radius des Rollkörpers, (v) die Flüssigkeitsschicht ist dünn und (vi) der Effekt der Oberflächenspannung ist vernachlässigbar. Die allgemeine Lösung des Problems beinhaltet den Zusammenhang der mechanischen Kräfte am Rollkörper (Normalkraft, Tangentialkraft, aufgebrachtes Drehmoment), dessen Winkelgeschwindigkeit, der Temperaturdifferenz zwischen dem Heizer und dem Medium mit Phasenwechsel und den thermophysikalischen Eigenschaften der flüssigen Phase. Einfachere Berechnungsmethoden werden für zwei Anwendungen entwickelt: (a) Schmelzvorgang eines Zylinders, der frei auf seiner Achse montiert ist und (b) Schmelzen eines sich drehenden Zylinders, dessen Achse stationär zur Heizfläche bleibt.

ПЛАВЛЕНИЕ ПРИ КОНТАКТЕ В ПРОЦЕССЕ ПРОКАТКИ

Аннотация—Рассматриваются основы теплопереноса в процессе плавления при прокатке, происходящем в узкой области контакта между телом, фазовое состояние которого изменяется, и твердым телом, играющим роль нагревателя. Теория основывается на следующих предположениях: (i) материал, фазовое состояние которого изменяется, находится при температуре плавления, (ii) поверхность твердого тела является изотермической, (iii) нагрев за счет трения в жидкой прослойке пренебрежимо мал, (iv) длина периметра жидкой области намного меньше радиуса ролика, (v) область жидкой прослойки тонка и (vi) поверхностное напряжение пренебрежимо мало. Построенное таким образом общее решение устанавливает связь между механической нагрузкой родика (нормальная и касательная составляющие силы, крутящий момент) и угловой скоростью его вращения, разностью температур между нагревателем и нагреваемым веществом, теплофизическими свойствами жидкой фазы. Разработаны более простые методы расчета для двух случаев: (а) плавления цилиндра, свободно закрепленного на своей оси и (б) плавления вращающегося цилиндра, ось которого неподвижна относительно поверхности нагревателя.